Carbohydrate Polymers 86 (2011) 1484–1490

Contents lists available at ScienceDirect

Carbohydrate Polymers

journal homepage: www.elsevier.com/locate/carbpol

Hydrogel containing hyaluronan and aliphatic oligo-carbonate moieties with tunable physical properties for potential application in protein release

Changjiang Fan, Jiaxing Tu, Xiaogang Yang, Liqiong Liao*, Lijian Liu

Department of Polymer Science, Wuhan University, Wuhan, Hubei 430072, PR China

ARTICLE INFO

Article history:
Received 14 March 2011
Received in revised form 15 June 2011
Accepted 15 June 2011
Available online 23 June 2011

Keywords:
Photopolymerization
Hyaluronan
2, 2-Dimethyltrimethylene carbonate
Poly(ethylene glycol)

ABSTRACT

Hyaluronan (HA) and aliphatic oligo-carbonate based biodegradable hydrogels were synthesized via photopolymerization of a methacrylated HA (HA-GMA) with oligo(2,2-dimethyltrimethylene carbonate)-block-poly(ethylene glycol)-block -oligo(2,2-dimethyltrimethylene carbonate) diacrylate (DPD-DA). Hydrogels with tunable physical properties such as swelling behavior, crosslink density, and mesh size were fabricated with different concentrations of HA-GMA or DPD-DA. Hydrogel–bovine serum albumin (BSA) construct was prepared by *in situ* photopolymerization. BSA release from the construct was evaluated *in vitro* and the release behavior can be controlled by adjusting the concentration of the precursors. By tailoring the concentration of different precursors in the hydrogels, more sustained release of BSA can be achieved (i.e., 120 h). The cytotoxicity of this novel hydrogel was also investigated and the hydrogel proved to be comparably cytocompatible to PEG hydrogels.

1. Introduction

Due to their excellent biocompatibility and similarity to mammalian tissue, hydrogels have been extensively investigated for applications in regenerative medicine research such as scaffolds in tissue engineering and matrices for bioactive drug deliveries (Carvalho, Coimbra, & Gama, 2009; Gombotz & Pettit, 1995; Lee & Yuk, 2007; Peppas, Hilt, Khademhosseini, & Langer, 2006; Slaughter, Khurshid, Fisher, Khademhosseini, & Peppas, 2009; Yin, Wang, Han, & Nie, 2010). Besides their bio-/chemical characteristics, the physical properties of the hydrogel such as water content, internal/external morphology, and permeability of water/nutrients play vital roles in their applications in regenerative medicine. Hydrogels with high equilibrium water content (EWC) and tunable physical properties are especially desirable in aforementioned applications. Those parameters can be tuned to meet specific requirements such as fast diffusion in/out of nutrients and wastes so as to achieve optimal cell growth and subsequent tissue regeneration (Leach & Schmidt, 2005).

Among those approaches that can be utilized to adjust the physical properties of hydrogel, copolymerization of different monomers/precursors is frequently used because of its versatility and wide applicability. Poly(ethylene glycol) (PEG) is a biocompatible, nontoxic, and nonimmunogenic water soluble polyether and is extensively studied as building blocks of hydrogels (Mellott, Searcy, & Pishko, 2001). The physical properties of PEG hydrogel can be tuned by changing the concentration or the molecular weight of precursor; however, PEG hydrogels are non-degradable under physiological condition, which has hindered its further applications in biomedical fields. Incorporation of biodegradable moieties into the PEG-based precursor has been very successful as an effort to introduce biodegradability to the hydrogel. Hubbell et al. (Sawhney, Pathak, & Hubbell, 1993) have synthesized a PEG triblock copolymer precursor with biodegradable poly(α-hydroxy acid) segments, and the hydrogel from this precursor proved to be biodegradable. Until now, aliphatic polyesters such as polylactide and poly(ε-caprolactone) have been investigated as biodegradable moieties in the PEG hydrogel. Poly(alkyl carbonate)s, such as poly(trimethylene carbonate) (PTMC) and poly(2, 2-dimethyltrimethylene carbonate) (PDTC), follow the slow surface erosion mechanism during their degradation; the degradation products (carbon oxide and diols) are considered to have less inflammatory response *in vivo* compared with those of poly(α-hydroxy acid)s (Habraken et al., 2008; Nair & Laurencin, 2007; Zhang, Kuijer, Bulstra, Grijpma, & Feijen, 2006). Zhang, Aung, Liao and Varghese (2009) reported a mechanically tough biodegradable hydrogel with a single precursor comprised of PEG and oligo(trimethylene carbonate) (oligo-TMC) segments. The cell culture results showed that the hydrogels based on PEG and TMC are biocompatible and did not exert any adverse effect on cells.

Hyaluronan (HA) is an important component in extracellular matrix (ECM) and can bind specifically to proteins in the ECM and on cell-surface receptors, regulate cell adhesion and motil-

* Corresponding author. Tel.: +86 27 87212246; fax: +86 27 68754067.
E-mail address: liqiongliao@hotmail.com (L. Liao).

0144-8617/$ – see front matter © 2011 Elsevier Ltd. All rights reserved.
doi:10.1016/j.carbpol.2011.06.048

ity, and mediate cell proliferation and differentiation (Chen & Abatangelo, 1999). In addition to its important role in many physiological processes, HA offers unique advantages such as being non-immunogenic and enzymatically degradable as a building block of biomaterials (Kirker, Luo, Nielson, Shelby, & Prestwich, 2002). However, the fast enzymatic degradation of HA *in vivo* has prevented it from exerting long-lasting effect in biomedical applications; many efforts have been made to lower the degradation rate of HA by chemical modification or chemical cross-linking (Burdick, Chung, Jia, Randolph, & Langer, 2005; Jeon et al., 2007; Leach, Bivens, Patrick, & Schmidt, 2003; Zhang et al., 2011).

The aim of this paper was to synthesize hydrogels with tunable physical properties through copolymerization of precursors based on PEG, oligo(2, 2-dimethyltrimethylene carbonate) (oligo-DTC), and HA. The influences of chemical composition of the hydrogels on their crosslink density, equilibrium water content, reswelling kinetics and interior morphology were evaluated. Hydrogel–bovine serum albumin (BSA) construct was successfully prepared by *in situ* photopolymerization and their release behavior was examined in details.

2. Experimental

2.1. Materials

DTC was synthesized according to the literature (Matsuo, Aoki, Sanda, & Endo, 1998; Sarel, Pohoryles, & Ben-Shoshan, 1959), recrystallized from anhydrous ethyl acetate for three times, and vacuum-dried before use. PEG with a molecular weight of 6000 g/mol (PEG6000, Shanghai Sinopharm Chemical Reagent Co., Ltd.) was purified by dissolution in dichloromethane (CH_2Cl_2) and precipitation in diethyl ether, the precipitate was dried in vacuum prior to use. Tin (II) 2-ethyl hexanoate ($Sn(Oct)_2$) was vacuum-distilled and dissolved in fresh anhydrous toluene. Acryloyl chloride was purified by distillation in the presence of hydroquinone. All the other reagents were used as received.

2.2. Synthesis of DTC

2,2-Dimethyl-1,3-propanediol (41.6 g, 0.4 mol) and ethyl chloroformate (86.8 g, 0.8 mol) were dissolved in 500 mL of anhydrous tetrahydrofuran (THF) in a round bottom flask at 0 °C, triethylamine (82.6 g, 0.816 mol) was added drop wise to the flask. The reaction mixture was stirred for 2 h at room temperature, and the white precipitate was filtered off. The solvent was removed from the filtrate by distillation under reduced pressure, then excessive diethyl ether was added to the filtrate and the product was crystallized at 0 °C.

2.3. Synthesis of DPD-DA

DTC, PEG6000 and 0.1% (mol/mol) $Sn(Oct)_2$ were charged into a glass ampoule and vacuum sealed (<50 Pa). The reaction mixture was heated in an oil bath at 140 °C for 24 h. After the reaction was completed, the reaction mixture was dissolved in 10 mL of chloroform ($CHCl_3$) and precipitated in excessive diethyl ether. The precipitate was collected by filtration and dried under vacuum at room temperature.

2.50 g of the polymerization product was dissolved in 100 mL of anhydrous toluene and dried by an azeotropic distillation. 0.2 g K_2CO_3 (Wang, Lu, Gruetzmacher, Currier, & Yaszemski, 2006) was added and then 0.12 mL acryloyl chloride in 10 mL CH_2Cl_2 was added drop wise at 0 °C. The reaction mixture was stirred overnight at 40 °C. The mixture was filtered and the filtrate was concentrated on a rotary evaporator and precipitated into diethyl ether. The white precipitate was collected and dried under vacuum at room temperature for 48 h. The chemical structure of the product was confirmed by ^{1}H NMR as DPD-DA.

2.4. Synthesis of HA-GMA

HA-GMA was synthesized according to literature with slight modification (Bencherif et al., 2008). Briefly, 1.00 g of HA ($M_n = 5 \times 10^5$ g/mol) was dissolved in a mixture of 200 mL of phosphate-buffered saline (PBS, pH 7.4) and 50 mL of N, N-dimethylformamide. Then 13.30 g of glycidyl methacrylate (GMA) and 6.70 g of triethylamine were added and stirred for five days, the solution was then precipitated twice in excessive acetone, filtered, dried under vacuum, and dialyzed for three days in distilled water.

2.5. Photopolymerization of precursor

The photopolymerization was carried out under 365 nm UV light according to the literature (Leach & Schmidt, 2005). Typically, a solution of HA-GMA, DPD-DA, Irgacure 2959 photoinitiator, with or without 2% BSA were prepared in phosphate-buffered saline (PBS); the solution was then transferred to a cylindrical molds (diameter 6 mm, height 4 mm) and subjected to photopolymerization under 365 nm UV at 0.8 mW/cm^2 for 30 min. After the polymerization, hydrogels was removed from the mold for further steps and characterizations.

2.6. ^{1}H NMR characterization and interior morphology

The ^{1}H NMR spectra of DPD-DA and HA-GMA were recorded on a Mercury VX-300 spectrometer using $CDCl_3$ and D_2O as solvents, respectively.

The synthesized hydrogels were first washed in distilled water for 48 h to remove un-reacted reactants, and then hydrogels were lyophilized. The dried hydrogels were fractured carefully in liquid nitrogen, sputter-coated with gold and subjected to observation under scanning electron microscopy (SEM, FEI-QUANTA 200, the Netherlands).

The width and height of each pore was measured manually and the mean value of width and height was defined as pore size.

2.7. Swelling behavior of hydrogels

The hydrogels were immersed in distilled water and swelled to equilibrium. The samples were weighed (W_{s0}) after blotting off the water on the surface and then dried under vacuum (W_{d0}). Five measurements were taken for each sample and the EWC was calculated by the following equation:

$$\mathrm{EWC}\% = \frac{W_{s0} - W_{d0}}{W_{s0}} \times 100$$

The vacuum-dried hydrogels were weighted (W_d) and immersed in distilled water. The samples were weighed at regular time intervals (W_t) until reaching swelling equilibrium (W_∞). The swelling ratio at time t was defined as follows:

$$\text{Reswelling ratio} = \frac{W_t}{W_d}$$

The equilibrium swelling ratio (ESR) was calculated by the following equation:

$$\mathrm{ESR} = \frac{W_\infty}{W_d}$$

2.8. Calculation of crosslink density

The crosslink density of hydrogels was calculated based on Flory–Rehner theory. The swelling ratio based on mass (Q_m) and swelling ratio based on volume (Q_v) of hydrogel were calculated with the following formulae (Marsano, Gagliardi, Ghioni, & Bianchi, 2000):

$$Q_m = \frac{W_{s0}}{W_{d0}}$$

$$Q_v = 1 + \frac{\rho_p}{\rho_s(Q_m - 1)}$$

where ρ_s is the density of the solvent (1 g/cm^3 for water) and ρ_p is the density of the dry polymer. ρ_p was calculated according to the method reported by Wieland, Houchin-Ray, & Shea (2007). Subsequently the average molecular weight between crosslinks (M_c) was calculated using a simplified Flory–Rehner equation (Flory, 1953; Metters, Anseth, & Bowman, 1999):

$$M_c = Q_v^{5/3}(0.5 - \chi)^{-1}\frac{V_1}{v}$$

where v is the specific volume of the dry polymer, V_1 is the molar volume of the solvent (18 cm^3/mol for water), and χ is the Flory polymer–solvent interaction parameter. The values of v and χ were calculated using the weighted average according to the composition of each hydrogel type (Wieland, Houchin-Ray, & Shea,2007). The χ value of PEG (0.426) was used as that of DPD-DA precursor, assuming that the presence of much shorter ODTC segments would not change the χ value significantly. The χ value of HA-GMA was 0.473 as described in literature.

The effective crosslink density (v_e) was then calculated as follows (Huglin, Rehab, & Zakaria, 1986):

$$v_e = \frac{\rho_p}{M_c}$$

2.9. Determination of diffusion coefficient

The diffusion coefficient (D_e) was determined using BSA, which is a widely used protein drug model. BSA was introduced into hydrogel in the photopolymerization process by adding predetermined amount of BSA to the polymerization mixture. The hydrogel–BSA construct was carefully transferred to 10 mL PBS in a 30 mL tube and incubated in a water bath at 37 °C. At specified time intervals, 0.5 mL of the solution was taken for analysis and the tube was replenished with 0.5 mL PBS solution. The BSA content in each solution was analyzed using the Bio-Rad protein assay (Leach & Schmidt, 2005). Measurements were done in triplicates and their average value was taken for calculation. The BSA mass released at time t (M_t) was calculated with the following formula (Leach & Schmidt, 2005):

$$M_t = C_t V + \sum C_{t-1} V_s$$

where C_t is the concentration of BSA in the release solution at time t, V is the total volume of release solution (10 mL), and V_s is the sample volume (0.5 mL).

2.10. Cell culture and cytotoxicity

HEK 293 T cells were culture in Dulbecco's Modified Eagle's Medium (DMEM high glucose, Hyclone) containing 2 mM glutamine complemented with 1.5 g/L sodium bicarbonate, 0.1 mM non-essential amino acids, 1.0 mM sodium pyruvate, and 10% fetal bovine serum (Hyclone) an incubator at 37 °C in the presence of 5% CO_2. Cells were trypsinized at 80% confluency using 0.05% trypsin and 0.02% EDTA in DMEM for seeding on the hydrogel surface. Cytotoxicity of the hydrogels was investigated via MTT assay (Park et al., 2007). Hydrogels were made by photopolymerization of 200 μL of corresponding precursor solutions on the bottom of wells of a 24-well plate. After the polymerization, the gels were washed with sterile PBS for 24 h, followed by sterilization in 70% ethanol for 12 h, then changed back to sterile PBS for 24 h; right before seeding HEK 293T cells, the gels were equilibrated with the culture medium for 12 h. 5×10^5 cells were then seeded in one well and incubated for 24 h, after which the medium was removed and the wells were washed with PBS twice, then 300 μL of MTT (0.5 g/L) solution in PBS was added into each well and incubated for 4 h. Hydrogel and MTT solution was transferred to a 15 mL eppendorf tube and tubes were centrifuged at 1000 rpm for 5 min. After removal of supernatant and hydrogels, 2 mL of DMSO was added and the tubes were shaken on a shaker at a speed of 100 rpm for 10 min at room temperature. Then the solution was centrifuged at 3000 rpm for 10 min, 40 μL of the supernatant for each sample was transferred to a 96-well plate, diluted to 200 μL with DMSO, and the absorbance was measured at 550 nm on a plate reader (Bio-tek Synergy MX, U.S.A.).

3. Results and discussion

3.1. Preparation of precursors

The chemical structure of the DPD-DA and HA-GMA precursor was characterized by ^{1}H NMR (Fig. 1). As shown in Fig. 1(a), the peaks at δ 4.10 ppm (–O–CH_2–) and δ 1.40 ppm (–CH_3) belong to protons in the repeating unit of the PDTC segment. The peak at δ 3.66 ppm (–CH_2–CH_2–O–) can be assigned to the repeating unit of PEG segment. The peaks at δ 5.86–6.44 ppm belong to protons in the diacrylate end group of DPD-DA and can be used to calculate the degree of acrylation of the precursor. The degree of polymerization of DTC in the DPD and DPD-DA precursors was 6, which was calculated from the relative integrals of proton peaks assigned to –CH_3 (δ 1.40 ppm) in oligo-DTC segment and –CH_2–CH_2–O– (δ 3.66 ppm) in PEG segment.

In Fig. 1(b), the peaks at δ 2.01 and δ 1.93 ppm belong to the methyl group of HA and GMA, respectively. The peaks at

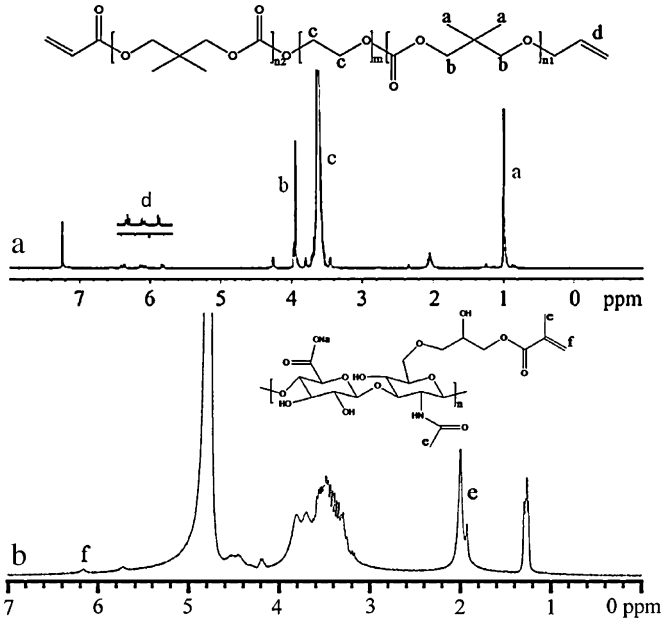

Fig. 1. ^{1}H NMR spectra of (a) DPD-DA and (b) HA-GMA.

Table 1
Physical properties of photopolymerized hydrogels.

Sample	HA-GMA (w/v%)	DPD-DA (w/v%)	ν_e (mol/m^3)	M_c (g/mol)	ESR	EWC (%)
Gel1	2	0	2.52 ± 0.02	490,400 ± 3121	37.9 ± 2.0	97.4 ± 5.3
Gel2	2	4	10.38 ± 0.22	111,700 ± 2187	27.2 ± 2.6	96.3 ± 8.8
Gel3	2	8	18.55 ± 0.28	63,200 ± 986	21.2 ± 1.9	95.3 ± 8.7
Gel4	0.2	8	22.32 ± 0.10	50,100 ± 203	20.3 ± 0.8	95.1 ± 4.2
Gel5	0.2	20	30.14 ± 0.19	38,500 ± 250	17.5 ± 0.2	94.3 ± 3.4

δ 5.75–6.10 ppm belong to the acrylate protons. The degree of methacrylation (DM) of HA-GMA was defined as the amount of methacryloyl groups per disaccharide in HA-GMA and calculated using the following equation:

$$\mathrm{DM} = \frac{3y}{2x - 3y}$$

where x is the relative peak integral of the methyl protons in HA-GMA, and y is the relative peak integral of the acrylate protons. The DM of HA-GMA was found to be 30%.

3.2. Physical properties of photopolymerized hydrogels

In addition to the covalent crosslink generated through free radical polymerization of acrylate groups in the precursors, the hydrophobic moieties, such as oligo-DTC segments in DPD-DA precursor and carbon–carbon single bond from methacrylate groups in HA-GMA can form clusters via hydrophobic interaction and contribute to the physical properties (Lin-Gibson, Jones, Washburn, Horkay, 2005). By adjusting the concentration of either DPD-DA or HA-GMA in the precursor solution, the physical properties of synthesized hydrogels (e.g., M_c and ν_e) can be altered remarkably (Table 1). For example, the crosslink density of Gel1, Gel2, and Gel3 increased from 2.52 to 18.55 mol/m^3 when the concentration of DPD-DA increased from 0 to 8% while keeping the same concentration of HA-GMA (2%). The M_c of the hydrogels decreased from 490,400 to 63,200 g/mol as a result of the increased crosslink density. At the same time, the ESR decreased from 37.9 to 21.2. The same trend was also observed on Gel4 and Gel5 at a lower concentration of HA-GMA (0.2%). It was also noticed that for Gel3 and Gel4, the crosslink density increased and the M_c decreased while lowering the concentration of HA-GMA, which was quite surprising. This could be attributed to the presence of negative charged COO^- groups in HA-GMA. The static charge repulsion between negative charged COO^- groups in hyaluronan can affect greatly the swelling ratio of hydrogel (Masters, Shah, Leinwand, & Anseth, 2005), thus slightly higher swelling ratio was observed with Gel3 which was synthesized from 2% of HA-GMA as compared to that of Gel4 from 0.2% HA-GMA. When the concentration of HA-GMA decreased to 0.2%, the effect of negative charge repulsion became less significant and led to decreased swelling ratio (21.2) and consequently increased crosslink density of 22.32 mol/m^3. It should be noted that the concentration of precursors and the hydrophobic interactions synergistically affect the swelling ratio and crosslink density of hydrogel. By carefully manipulating of these factors, the properties of hydrogel can be fine tuned to meet various criteria in the biomedical applications.

Fig. 2 shows the re-swelling kinetics profiles of the hydrogels in distilled water. All swelling kinetic curves are plotted as the mean value of three samples and almost all hydrogels reached equilibrium within 30 min and the EWC was higher than 90% for all the hydrogels. In the early stage of swelling in distilled water, the dried hydrogels were quickly swollen, but the swelling rate (slopes of swelling kinetics) became smaller from Gel1 to Gel5, which was consistent with the result that the surface area decreased gradually from Gel1 to Gel5 presented in Fig. 2. It is no doubt that with increasing the concentration of DPD-DA and decreasing the concentration of HA-GMA in the polymerization mixture, the hydrogel would exhibit increased crosslink density and thus the diffusion of solvent was hindered.

3.3. Interior morphology

The interior morphology of the hydrogels is displayed in Fig. 3. All the SEM images show three-dimensional macroporous structure for each type of hydrogel. But they also clearly illustrate the dependence of interior morphology of the hydrogels on the composition ratio of DPD-DA to HA-GMA. With increasing the ratio of DPD-DA to HA-GMA from Gel1 to Gel5, the pore structure changed from an irregular round shape having wavy thin walls to a well-defined structure having thick wall (Fig. 2). The average pore sizes for Gel1, Gel2, Gel3, Gel4, and Gel5 were 190, 120, 100, 80, and 60 μm, respectively, which follow the same trend in the crosslink density of these gels.

3.4. Protein release behavior

The protein release behavior of the hydrogels was investigated using BSA as the model drug. The release profiles of hydrogel–BSA constructs in PBS (pH 7.4) at 37 °C are shown in Fig. 4. Hydrogel with lower crosslink density usually accompanies larger mesh size, which would allow faster mass transfer through the hydrogel network. The release rate of BSA from the constructs decreased from Gel1 to Gel5 with the increase of the crosslink density of the hydrogels (Table 2). As shown in Fig. 4(a), the cumulative release at 6 h was 90.8%, 88.6%, and 86.9% for Gel1, Gel2, and Gel3, respectively. Gel1, Gel2, and Gel3 exhibited fast release of BSA and the release rate in different constructs followed the trend of Gel1 > Gel2 > Gel3, which was in good agreement with the trend of hydrogel mesh size. The same phenomenon was also observed for Gel4 and Gel5

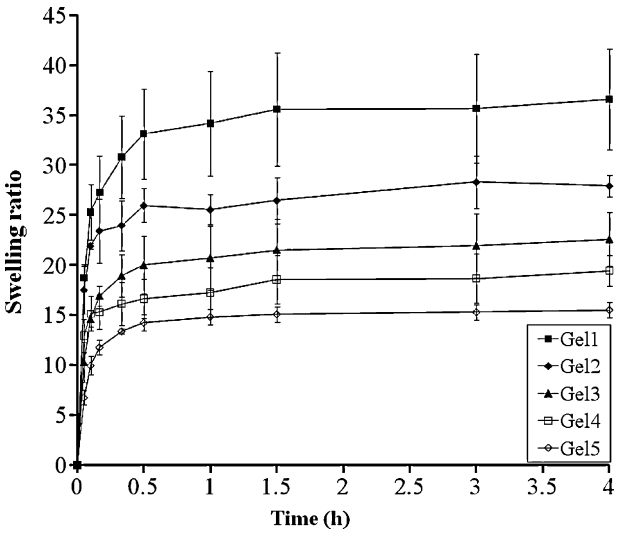

Fig. 2. Reswelling kinetics of the hydrogels in distilled water.

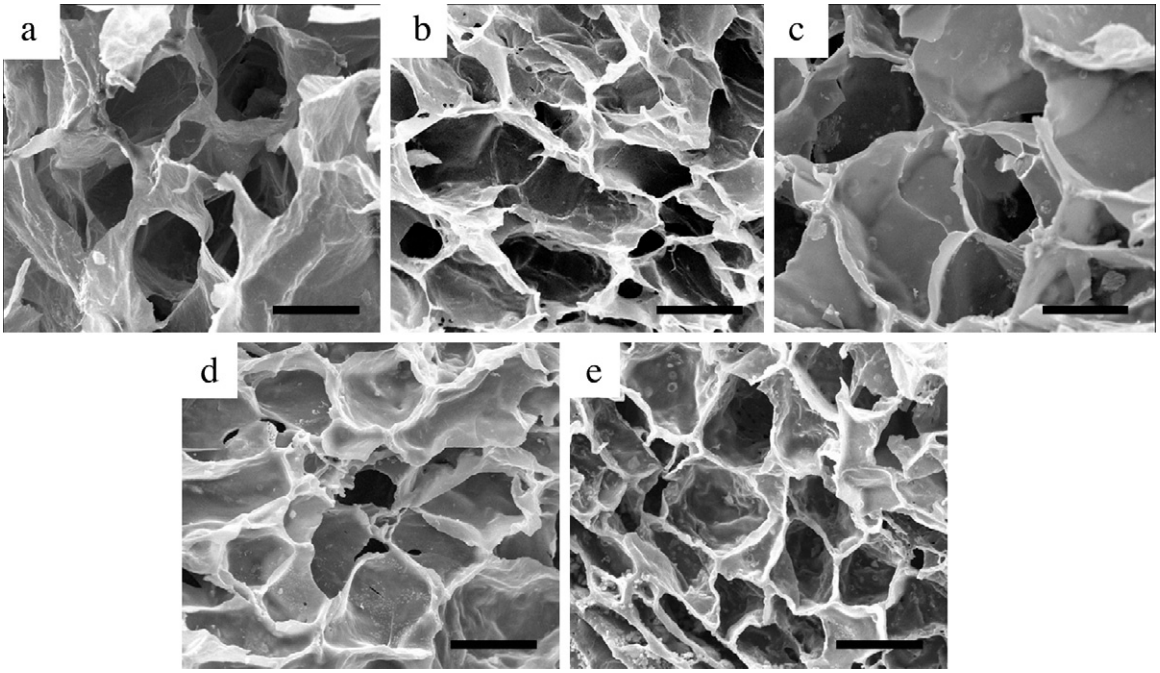

Fig. 3. SEM images of the hydrogels: (a) Gel1, (b) Gel2, (c) Gel3, (d) Gel4, and (e) Gel5. The scale bar represents 100 μm.

(Fig. 4(b)). Similarly, change in the concentration of HA-GMA also affects the BSA release behavior. When the concentration of HA-GMA decreased from 2% to 0.2%, prolonged release was achieved. The cumulative release at 6 h was 52.4% for Gel4, which was much lower than that of Gel3 (86.9%). It took almost 120 h for 89.0% of BSA to be released from Gel4. By tailoring the concentration of oligo-DTC-PEG-oligo-ODTC or HA moiety in the hydrogels, more sustained release of BSA can be achieved.

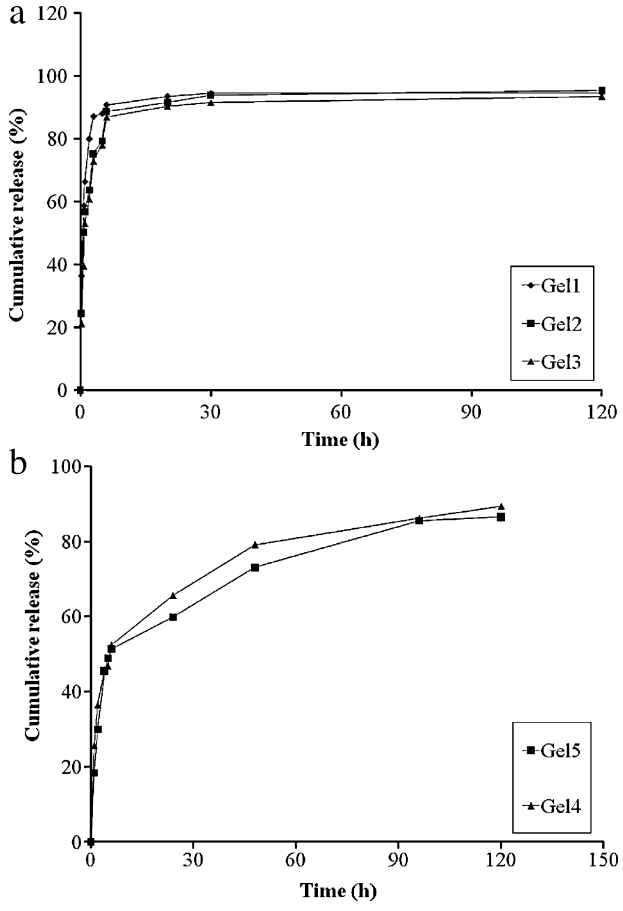

Fig. 4. *In vitro* release profiles of hydrogels–BSA construct in PBS (pH 7.4) at 37 °C.

We next plotted the mean value of cumulative release of BSA against the square root of release time at cumulative release lower than 60% (Fig. 5), good linear correlation ($R^2 > 0.99$) was found for each hydrogel. According to the Ritger–Peppas equation: $M_t/M_\infty = kt^n$ (k is a kinetic constant, t is the release time) (Ritger & Peppas, 1987), n equals to 1/2 only if the BSA release is Fickian diffusion governed. The linear relationship between the cumulative release and the square root of release time suggests that BSA release from this hydrogel is governed by Fickian diffusion and implies that the mesh size of the hydrogel was larger than the hydrodynamic diameter of BSA in solution (Carvalho, Coimbra, & Gama, 2009; Censi, Fieten, Hennink, & Vermonden, 2010).

The approximation equation of Fick's second law was then applied to calculate the effective protein diffusion coefficient (D_e) in the early release stage (Leach & Schmidt, 2005; Ritger & Peppas, 1987):

$$\frac{M_t}{M_\infty} = 4\left(\frac{D_e t}{\pi \delta^2}\right)^{1/2}$$

where M_∞ is cumulative mass of released protein after two weeks, M_t/M_∞ represents the fractional mass of released protein, D_e is the effective diffusion coefficient, t is the release time, and δ is the hydrogel thickness.

Table 2
Calculations of D_e for BSA of the hydrogels.

Sample	$D_e \times 10^7$ (cm^2/s)	D_e/D_0
Gel1	1.50 ± 0.23	0.164 ± 0.025
Gel2	0.90 ± 0.11	0.098 ± 0.012
Gel3	0.61 ± 0.16	0.066 ± 0.018
Gel4	0.34 ± 0.07	0.037 ± 0.008
Gel5	0.28 ± 0.10	0.031 ± 0.011

D_0 and D_e/D_0 are defined as infinite-dilution diffusion coefficient and normalized diffusivity respectively, and D_0 for BSA in water at 37 °C is 9.14×10^{-7} cm^2/s (Censi, Fieten, Hennink, & Vermonden, 2010; Leach & Schmidt, 2005).

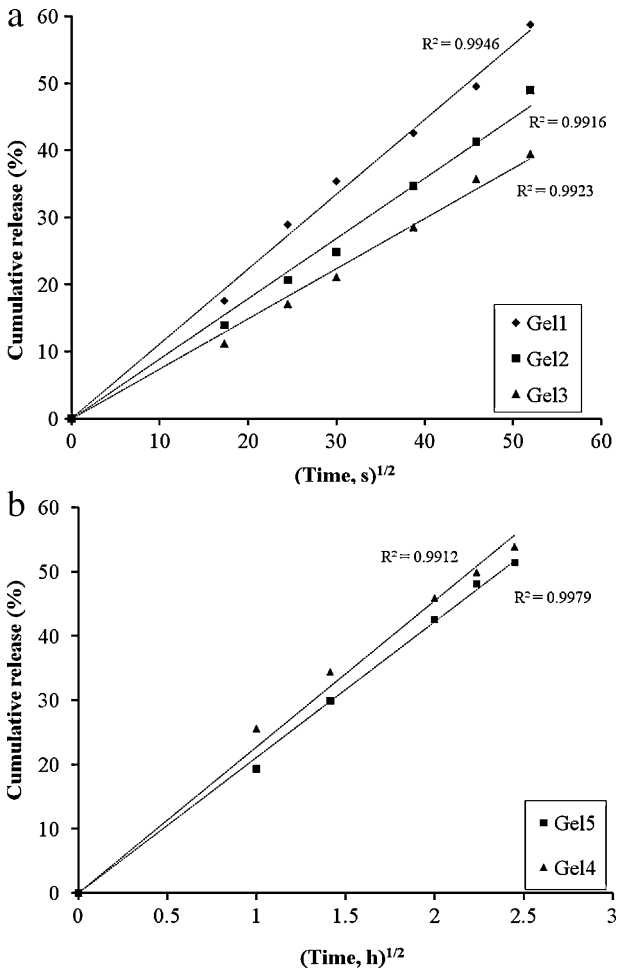

Fig. 5. Release kinetics of the hydrogels as a function of the square root of time.

The slopes of trend lines in Fig. 5 were used to calculate the D_e and D_e/D_0 of each type of hydrogel (Table 2). From Gel1 to Gel5, the value of D_e and D_e/D_0 for BSA decreased dramatically from 1.50×10^7 to 0.28×10^7 cm^2/s and from 0.164 to 0.031, respectively. The decreasing diffusion coefficient of hydrogels further demonstrated that by changing the precursor concentration, not only physical properties of hydrogels can be tuned, but also controlled drug release can be achieved. This hydrogel can be a potential matrix for sustained protein drug release.

3.5. Cytotoxicity of hydrogel

MTT assay was performed to investigate the cytocompatibility of this novel hydrogels. Since hydrogels made from PEG3400 has been widely used as drug delivery carrier and tissue engineering scaffolds due to its excellent cytocompatibility, we used a hydrogel synthesized from PEGDA 3400 as a control to study the cytotoxicity of the novel hydrogel. As shown in Fig. 6, no statistically significant difference in absorbance at 550 nm was observed between the control and the novel hydrogels (Gel3 and Gel4) after 1 day of culture. This result suggests that oligo(2,2-dimethyltrimethylene carbonate) and GMA portions along with the presence of HA did not exert adverse effect on HEK 293T cells. This novel hydrogel showed comparable cytotoxicity with the widely recognized PEG hydrogels, and could be used safely in protein delivery or other biomedical applications.

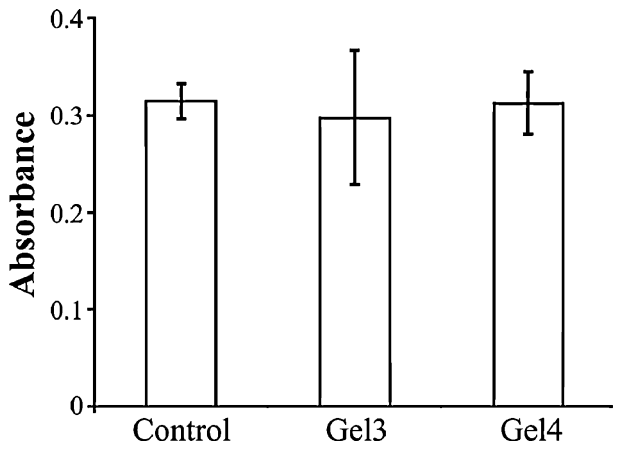

Fig. 6. Viability of HEK 293T cells cultured for 24 h on the pure PEG hydrogels, Gel3, and Gel4.

4. Conclusion

A series of hydrogels were successfully prepared by photo-copolymerization of an oligo-DTC based precursor and HA-GMA. All the hydrogels showed three-dimensional macroporous structure and the physical properties of the hydrogel can be tuned by adjusting the concentration of the precursors. Both the concentration of precursors and the hydrophobic interactions synergistically have influence on the crosslink density of hydrogel. With the increase of the crosslink density of the hydrogel, the release rate of BSA from the hydrogel–BSA constructs decreased due to the decrease of the BSA diffusion coefficient. This novel hydrogel system has showed its biocompatibility and could be potentially used in controlled protein release.

Acknowledgements

The authors are grateful to the financial support of the National Natural Science Foundation of China (Grant no. 20904042) and the Fundamental Research Funds for the Central Universities (Grant no. 2082005).

References

Bencherif, S. A., Srinivasan, A., Horkay, F., Hollinger, J. O., Matyjaszewski, K., & Washburn, N. R. (2008). Influence of the degree of methacrylation on hyaluronic acid hydrogels properties. *Biomaterials*, *29*, 1739–1749.

Burdick, J. A., Chung, C., Jia, X. Q., Randolph, M. A., & Langer, R. (2005). Controlled degradation and mechanical behavior of photopolymerized hyaluronic acid networks. *Biomacromolecules*, *6*, 386–391.

Carvalho, J. M., Coimbra, M. A., & Gama, F. M. (2009). New dextrin–vinylacrylate hydrogel: Studies on protein diffusion and release. *Carbohydrate Polymers*, *75*, 322–327.

Censi, R., Fieten, P. J., Hennink, W. E., & Vermonden, T. (2010). In situ forming hydrogels by tandem thermal gelling and Michael addition reaction between thermosensitive triblock copolymers and thiolated hyaluronan. *Macromolecules*, *43*, 5771–5778.

Chen, W. Y. J., & Abatangelo, G. (1999). Functions of hyaluronan in wound repair. *Wound Repair and Regeneration*, *7*, 79–89.

Flory, P. J. (1953). *Principles of polymer chemistry*. Ithaca, NY: Cornell University Press.

Gombotz, W. R., & Pettit, D. K. (1995). Biodegradable polymers for protein and peptide drug delivery. *Bioconjugate Chemistry*, *6*, 332–351.

Habraken, W. J. E. M., Zhang, Z., Wolke, J. G. C., Grijpma, D. W., Mikos, A. G., Feijen, J., et al. (2008). Introduction of enzymatically degradable poly(trimethylene carbonate) microspheres into an injectable calcium phosphate cement. *Biomaterials*, *29*, 2464–2476.

Huglin, M. B., Rehab, M. M. A. M., & Zakaria, M. B. (1986). Thermodynamic interactions in copolymeric hydrogels. *Macromolecules*, *19*, 2986–2991.

Jeon, O., Song, S. U., Lee, K. J., Park, M. H., Lee, S. H., Hahn, S. K., et al. (2007). Mechanical properties and degradation behaviors of hyaluronic acid hydrogels cross-linked at various cross-linking densities. *Carbohydrate Polymers*, *70*, 251–257.

Kirker, K. R., Luo, Y., Nielson, J. H., Shelby, J., & Prestwich, G. D. (2002). Glycosaminoglycan hydrogel films as bio-interactive dressings for wound healing. *Biomaterials*, *23*, 3661–3671.

Leach, J. B., Bivens, K. A., Patrick, C. W., & Schmidt, J. C. E. (2003). Photocrosslinked hyaluronic acid hydrogels: Natural, biodegradable tissue engineering scaffolds. *Biotechnology and Bioengineering*, *82*, 578–589.

Leach, J. B., & Schmidt, C. E. (2005). Characterization of protein release from photocrosslinkable hyaluronic acid–polyethylene glycol hydrogel tissue engineering scaffolds. *Biomaterials*, *26*, 125–135.

Lee, K. Y., & Yuk, S. H. (2007). Polymeric protein delivery systems. *Progress in Polymer Science*, *32*, 669–697.

Lin-Gibson, S., Jones, R. L., Washburn, N. R., & Horkay, F. (2005). Structure–property relationships of photopolymerizable poly(ethylene glycol) dimethacrylate hydrogels. *Macromolecules*, *38*, 2897–2902.

Marsano, E., Gagliardi, S., Ghioni, & Bianchi, E. (2000). Behaviour of gels based on (hydroxypropyl) cellulose methacrylate. *Polymer*, *41*, 7691–7698.

Masters, K. S., Shah, D. N., Leinwand, L. A., & Anseth, K. S. (2005). Crosslinked hyaluronan scaffolds as a biologically active carrier for valvular interstitial cells. *Biomaterials*, *26*, 2517–2525.

Matsuo, J., Aoki, K., Sanda, F., & Endo, T. (1998). Substituent effect on the anionic equilibrium polymerization of six-membered cyclic carbonates. *Macromolecules*, *31*, 4432–4438.

Mellott, M. B., Searcy, K., & Pishko, M. V. (2001). Release of protein from highly cross-linked hydrogels of poly(ethylene glycol) diacrylate fabricated by UV polymerization. *Biomaterials*, *22*, 929–941.

Metters, A. T., Anseth, K. S., & Bowman CN. (1999). Fundamental studies of biodegradable hydrogels as cartilage replacement materials. *Biomedical Science Instrumentation*, *35*, 33–38.

Nair, L. S., & Laurencin, C. T. (2007). Biodegradable polymers as biomaterials. *Progress in Polymer Science*, *32*, 762–798.

Park, J. S., Woo, D. G., Sun, B. K., Chung, H. M., Im, S. J., Choi, Y. M., et al. (2007). In vitro and in vivo test of PEG/PCL-based hydrogel scaffold for cell delivery application. *Journal of Controlled Release*, *124*, 51–59.

Peppas, N. A., Hilt, J. Z., Khademhosseini, A., & Langer, R. (2006). Hydrogels in biology and medicine: From molecular principles to bionanotechnology. *Advanced Materials*, *18*, 1345–1360.

Ritger, P. L., & Peppas, N. A. (1987). A simple equation for description of solute release II. Fickian and anomalous release from swellable devices. *Journal of Controlled Release*, *5*, 37–42.

Sarel, S., Pohoryles, L. A., & Ben-Shoshan, R. (1959). Organic carbonates IV. Factors affecting formation of homologous cyclic carbonates. *The Journal of Organic Chemistry*, *24*, 1873–1878.

Sawhney, A. S., Pathak, C. P., & Hubbell, J. A. (1993). Bioerodible hydrogels based on photopolymerized poly(ethylene glycol)-co-poly(α-hydroxy acid) diacrylate macromers. *Macromolecules*, *26*, 581–587.

Slaughter, B. V., Khurshid, S. S., Fisher, O. Z., Khademhosseini, A., & Peppas, N. A. (2009). Hydrogels in regenerative medicine. *Advanced Materials*, *21*, 3307–3329.

Wang, S. F., Lu, L. C., Gruetzmacher, J. A., Currier, B. L., & Yaszemski, M. J. (2006). Synthesis and characterizations of biodegradable and crosslinkable poly(α-caprolactone fumarate), poly(ethylene glycol fumarate), and their amphiphilic copolymer. *Biomaterials*, *27*, 832–841.

Wieland, J. A., Houchin-Ray, T. L., & Shea, L. D. (2007). Non-viral vector delivery from PEG–hyaluronic acid hydrogels. *Journal of Controlled Release*, *120*, 233–241.

Yin, R. X., Wang, K. M., Han, J., & Nie, J. (2010). Photo-crosslinked glucose-sensitive hydrogels based on methacrylate modified dextran-concanavalin A and PEG dimethacrylate. *Carbohydrate Polymers*, *82*, 412–418.

Zhang, C., Aung, A., Liao, L. Q., & Varghese, S. (2009). A novel single precursor-based biodegradable hydrogel with enhanced mechanical properties. *Soft Matter*, *5*, 3831–3834.

Zhang, Z., Kuijer, R., Bulstra, S. K., Grijpma, D. W., & Feijen, J. (2006). The in vivo and in vitro degradation behavior of poly(trimethylene carbonate). *Biomaterials*, *27*, 1741–1748.

Zhang, L., Li, K. F., Xiao, W. Q., Zheng, L., Xiao, Y. M., Fan, H. S., et al. (2011). Preparation of collagen–chondroitin sulfate–hyaluronic acid hybrid hydrogel scaffolds and cell compatibility in vitro. *Carbohydrate Polymers*, *84*, 118–125.